

Article

The Effect of a Blended Polycarboxylate Superplasticizer on the Rheology of Self-Compacting Concrete Paste

Maverick Swartz ¹, Willy Mbasha ^{1,2} and Rainer Haldenwang ^{1,*}

¹ Department of Civil Engineering and Geomatics, Cape Peninsula University of Technology, Bellville 7530, South Africa

² PPC DR Congo, Kinshasa, Democratic Republic of the Congo

* Correspondence: haldenwangr@cput.ac.za; Tel.: +27-834-572-382

Abstract: High-strength-performing concretes (HSPC) have been used extensively due to new building requirements and their special properties suitable for modern cities. Superplasticizers (SPs) are essential components in the mix design of these concretes since they control their fresh properties and improve durability. In practice, superplasticizers are used to achieve a desired workability without increasing the water content by dispersing agglomerated cement particles. The aim of this research was to investigate the effectiveness of a blended polycarboxylate (PCE) superplasticizer on the rheological behavior for three different cements. It was found that two SP agents with the same molecular structure but with different weight and side-chain length provided an SP product that had a greater effect on the rheological properties of the cement paste. Yield stress values remained unaffected in the presence of blended SP with an SP fraction above 50% and with long side chains while its adsorption ability increased with the decrease in SP fraction with shorter side chains and lower molecular mass.

Keywords: self-compacting concrete paste; adsorption; mini-slump; blended polycarboxylate; rheometer; sulphate-sensitivity; competitive adsorption



Citation: Swartz, M.; Mbasha, W.; Haldenwang, R. The Effect of a Blended Polycarboxylate Superplasticizer on the Rheology of Self-Compacting Concrete Paste. *Appl. Sci.* **2023**, *13*, 4148. <https://doi.org/10.3390/app13074148>

Academic Editors: Seung-Yup Jang and Seung-Jun Kwon

Received: 22 February 2023

Revised: 17 March 2023

Accepted: 22 March 2023

Published: 24 March 2023



Copyright: © 2023 by the authors. Licensee MDPI, Basel, Switzerland. This article is an open access article distributed under the terms and conditions of the Creative Commons Attribution (CC BY) license (<https://creativecommons.org/licenses/by/4.0/>).

1. Introduction

Self-compacting concrete (SCC) is a concrete that compacts under its own weight without any mechanical intervention, such as conventional vibrating or poking techniques, to achieve optimum compaction. It is difficult for traditional concrete to achieve self-compaction due to its cohesiveness nature. One way to reach the desired workability is to add more water to the mix; however, this compromises the strength of the concrete by creating more pores within the hydrating network [1]. In self-compacting concrete, workability is defined as the ability for fresh concrete to be easily applied without segregation [2].

Fluidity is considered essential when classifying SCC. One of the methods used to reach the desired fluidity without adding additional water is to add a viscosity modifying admixture such as a high-range water-reducing agent (HRWRA), or superplasticizer [3–6]. These (HRWRAs) increase the workability of a fresh concrete mix by dispersing flocculated cement particles which entrap free water molecules within the concrete system. Among commercially available SPs, polycarboxylates (PCE) and naphthalene sulfonate formaldehyde (NSF) SPs are preferred in the cement industry, with PCE based SPs being the most popular [5].

PCE SPs have a comb-like structure which consist of a polyanionic backbone, which is mainly methacrylate, partially esterified with grafted neutral side chains of polyethylene oxide units (PEO) [3,7,8]. The negatively charged backbone of the PCE-based SP adsorbs onto the positive surface of the hydrating products of the cement particles resulting in a more fluid concrete mix. The long polyethylene oxide (PEO) side chains cause steric hindrance effects by dispersing cement particles within the solution through steric repulsion mechanisms [8–10].

Tricalcium aluminate (C_3A) is a cement phase that reacts more actively with water, resulting in hydrate products which are responsible for the initial setting of the fresh concrete mix. The adsorption ability and effectiveness of a superplasticizer in cement systems largely depends on its interaction with the aluminate phase [11]. During the hydration period, the adsorption of SP onto cement particles reaches the saturation state resulting in non-adsorbed SP being dispersed within the solution and, thus, increasing the fluidity of the fresh mixture [9,11].

Previous Research on the Blending of Material

Li et al. [12] observed the flow behavior of cement pastes by adding aminosulfonic acid-based SPs (AS) within cement systems containing two retarders including sodium gluconate (SG) and citric acid (CN). They reported a reduction in adsorption of AS in the presence of these two retarders, mostly due to the unavailability of reaction sites within the cement systems. Yoon and Kim [13] observed the effect of three PCE polymers on the fluidity of a cement paste, using a mini-slump test. They simultaneously added three PCE polymers to the same paste and reported increases in slump loss of cement pastes containing multiple SPs compared to those with only one PCE polymer. However, a higher SP adsorption was achieved in these mixtures, suggesting that the non-adsorbed polymers increased the fluidity of the system, thus causing slump loss, and the steric hindrance between polymers prevented further adsorption.

Matsuzawa et al. [14] investigated the effect of non-adsorbing SPs on the fluidity of cement pastes containing silica fume by comparing the degree of SP adsorptions and subsequent impact on their rheological behavior. They used eight PCE SPs with an average molecular weight of approximately 10,000 g/mol, differentiated only by the lengths of their side chains. The adsorption was determined by the total organic carbon content utilizing the depletion method, and the rheological results were determined using a rotational cylinder viscometer with cup and bob. It was concluded that SPs containing higher COO^- units exhibited a higher degree of adsorption while the fluidity of the corresponding paste was more dependent on the length of the side chains of the non-adsorbed SP. Superplasticizers with longer side chains tended to increase the fluidity of the cement pastes following the larger hindrance effect within the medium.

It is, therefore, understood that the dispersing ability of a PCE-based SP is highly dependent on the adsorption ability and effectiveness thereof, which determines the fluidity of a fresh concrete mixture. The difference in the adsorption ability is also dependent on the chemical composition of the cement particles because of the affinity the SP has towards the aluminate phases, which leaves room for further investigation [9].

In practice, HRWRAs are produced by blending two agents based on the effect it has on the cement workability [13]. However, the effect of competitive adsorption between multiple SP polymers with different molecular structures when simultaneously added to the same mixture has not been fully explored [15]. This work investigated the effectiveness of a blended PCE polymer on the rheological behavior of different cement pastes with distinct chemical compositions.

2. Materials and Methods

2.1. Material Used

Three different Portland cements of CEM II type were all produced by the same company but at different factories. The two SPs used were different polycarboxylate SPs which differed in polymer length and molecular weight.

2.2. Cement Composition

The chemical analysis was done by X-ray fluorescence analysis (XRF) to determine the oxide composition of the three cements under investigation. The chemical composition of the cements used is presented in Table 1.

Table 1. Chemical Analysis of the cements used.

Chemical Oxides (%)	Cement		
	Cement 1	Cement 2	Cement 3
SiO ₂	22.6	19.9	20.2
Al ₂ O ₃	3.07	4.14	4.47
Fe ₂ O ₃	4.83	2.89	3.06
Mn ₂ O ₃	0.09	0.06	0.67
TiO ₂	0.39	0.24	0.28
CaO	63.46	65.66	63.72
MgO	1.52	0.90	2.62
P ₂ O ₅	0.08	0.12	0.05
SO ₃	2.51	2.46	3.53
Cl	0.00	0.00	0.00
K ₂ O	0.49	0.70	0.22
Na ₂ O	0.28	0.16	0.06
LOI	1.45	3.05	1.99
Total	100.8	100.3	100.9

2.3. Physical Properties of the Cement Used

The physical properties of the cements used are presented in Table 2.

Table 2. Physical properties of the cement used.

Physical Testing	Cement		
	Cement 1	Cement 2	Cement 3
Relative Density	3.09	3.15	3.12
Specific Surface, cm ² /g	3800	4300	4100
Standard Consistency, %	28.0	27.6	28.0
Initial Set Min	180	130	100
Final Set Min	195	150	120
32 µm Residue, %	15.6	23.2	9.5
45 µm Residue, %	5.3	10.3	2.2
90 µm Residue, %	0.2	0.8	0.1
212 µm Residue, %	0.0	0.1	0.0

2.4. Superplasticizer

This section describes the characteristics of the SP used in this investigation by providing a comparison in Table 3 and by using the FTIR results to confirm the description provided by the suppliers of the admixtures.

Table 3. Characteristics of Superplasticizer.

Characteristics	SP-A	SP-B
Consistency	Liquid	Liquid
Color	Amber	Amber
Density according to ISO 758 (g/cm ³)	1.08 ± 0.02	1.07 ± 0.02
Dry content according to EN 480-8 (%)	30.5 ± 1.5	30 ± 1.5
Chlorides soluble in water according to EN 480-10 (%)	<0.1	<0.1
Alkali content (Na ₂ O equivalent) according to EN 480-12 (%)	<3	<2.5

2.5. Characterising the Superplasticizers

The SPs used for this project were named SP-A and SP-B, and are two PCE polymers used for multiple applications in industry. Both SPs were prepared by radical polymerization and are based on Methacrylic acid MPEG-Methacrylate. The molecular weights of the two polymers as received from the suppliers are as follows:

- SP-A = 42,000 (g/mol)
- SP-B = 40,000 (g/mol)

SP-A is a high negatively charged polymer with a non-ionic backbone consisting of long thin side chains, which results in a strong affinity towards the surface of the cement particles through electrostatic adhesion, ensuring high mechanical resistance for shorter periods.

SP-B is a lower negatively charged polymer with a non-ionic backbone consisting of shorter and thicker side chains, resulting in a slower adhesion to cement particles providing moderate mechanical resistance for longer periods.

The peaks of the graph in Figure 1 were considered for the calculation used by Janowska-Renkas (2013) [16] to define the hydrophilicity of the side chains using FTIR results of the two admixtures. The ratio between the hydrophilic Ester groups and the hydrophobic Ether groups of the PCE structure is used to determine the hydrophilicity of the side chains. The first method used the absorbance from the peaks (Ether absorbance/Ester absorbance) to calculate the hydrophilicity and the second method used the area of the peaks (Ether area/Ester area). Equation (1) was then used to calculate the absorbance from the transmittances. It was determined that both methods used confirm the assumption made about the polymers and established that SP-A has a greater hydrophilic nature compared to SP-B, which translates to SP-A being, theoretically, more efficient in increasing fluidity because of its longer side chains.

$$A = -\log \frac{P_T}{P_O} \tag{1}$$

$$\text{Hydrophilicity} = (A_{ET}^{1080} / A_{ES}^{1640}) \tag{2}$$

$$\text{Hydrophilicity} = (\text{Area}_{ET}^{1080} / \text{Area}_{ES}^{1640}) \tag{3}$$

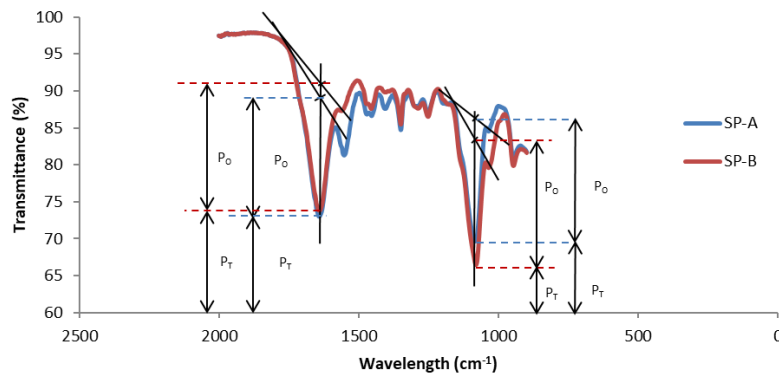


Figure 1. FTIR Spectrum of SP-A and SP-B (2000–900 cm⁻¹).

2.6. Blending Process of the PCE SP

SP-C consisted of a blend of two different PCE SPs, SP-A and SP-B, which were blended at predetermined ratios where SP-C will indicate x% of SP-A in SP-C, and the difference is y% of the SP-B fraction at an optimum dosage of 0.25%.

2.7. Experimental Equipment and Procedure

2.7.1. Sample Preparation

The sample preparation was just before testing to prevent contamination and all the tests were done at paste scale with a water/cement ratio of 0.45. A digital scale was used to weigh the 100 g of cement and 45 g of distilled water. The water was adjusted to accommodate for the presence of the SP. The SP was added to the water using a syringe to measure dosages accurately, and then stirred to homogenize the SP and water mixture before adding it to the dry cement. The mixture was immediately homogenized with a mixing tool for two minutes and testing followed directly thereafter.

2.7.2. Optimization of the SP-C Blend

SP-A and SP-B were added separately to each cement at dosages of 0.1% to 0.8% by weight of the cement, at a rate of 0.1%, and tested with the rheometer by applying hysteresis loops and fitting the downward curve to the Bingham model to determine the yield stress from the y-intercept. The optimum dosage was observed to be the SP dosage that had no noticeable effect on the yield stress value with further increase in SP.

2.7.3. Rheometer

An Anton Paar MCR 51 rotational rheometer with 50 mm diameter roughened parallel plates and a gap of 0.6 mm was used to determine the rheological parameters (yield stress and viscosity) of the fresh cement paste. A shear rate ramp was applied to the paste sample and the rheological properties were extrapolated from applying the Bingham model to the downward curve of the hysteresis loop measurement. The hysteresis loop consists of two branches of measurements which starts at a shear rate of 0.1 s^{-1} and ends at 100 s^{-1} , and then the shear rate decreases from 100 s^{-1} back to 0.1 s^{-1} . The rheometer recorded measurements at 10 intervals going up, and at 10 intervals coming down with a test duration of 300 s per test (15 s per measuring point). Before the start of each test, the cement sample was first pre-sheared at a shear rate of 50 s^{-1} for 10 s to break down any network of agglomerates that could have formed at the start of the measurement. The Bingham model was fitted to the downward curve data to obtain the yield stress (y-intercept) and viscosity (slope) [17,18]. The Bingham model is as follows:

$$\tau_y = \tau_0 + \mu_p \dot{\gamma} \quad (4)$$

where τ_y is the yield stress (Pa), μ_p is the Bingham plastic viscosity (Pa·s) and $\dot{\gamma}$ is the shear rate (1/s).

The 100 g cement powder was weighed on a digital scale, and 44.75 g of distilled water was weighed to accommodate the percentage of SP used. The SP was added to the distilled water by using a syringe at a percentage w.r.t the weight of the cement. The distilled water (with SP) was added to the cement powder and was immediately mixed for two minutes before moving the sample to the rheometer for measurement. The sample was trimmed and covered with a sample protection cell to control the test temperature and to prevent the sample from losing water through evaporation during the shearing process. The temperature controlling bath attached to the rheometer was used to maintain the temperature at $25 \text{ }^\circ\text{C}$ [17,19]. After each test, the parallel plates of the rheometer were wiped clean in preparation for the next sample. This procedure was followed for all the measurements at different SP dosages.

2.7.4. Mini-Slump Test

The mini-slump test (Figure 2) was used to determine the loss of workability of the fresh cement paste by observing the diameter of the spread over time. The fresh cement was prepared in the same way as for the rheometer tests.

Previous studies showed that there is a relationship between the slump diameter and the yield stress. This makes the mini-slump test a suitable empirical test for measuring the yield stress of low viscosity cement mixtures [7]. The slump measurements can be used to determine the yield stress by making use of the following equation [3]:

$$\tau_y = \frac{225\rho gV^2}{128\pi^2 R^2 \left(1 + \frac{225}{128\pi} \sqrt{3VR^{-3}}\right)} - \lambda \frac{R^2}{V} \quad (5)$$

where:

- τ_y = shear stress (Pa)
- ρ = paste density (kg/m^3)

- R = average spread diameter (m)
- λ = a parameter fixed at 0.003, that takes into account the liquid–vapor interfacial energy and the wet angle
- V = volume of the cone (m^3)

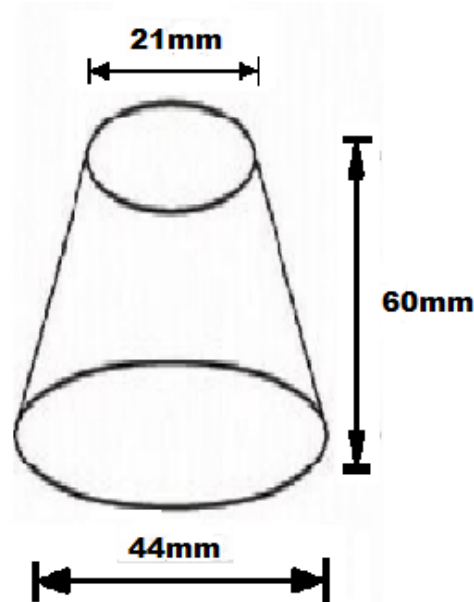


Figure 2. Dimensions of the mini-slump cone.

The fresh cement paste was poured in the top opening of the cone and allowed to set for 30 s before slowly lifting the cone vertically, being careful to prevent the effect of inertia. The time is recorded from the moment the cone is lifted until the flow of the spread has come to a complete stop. The orthogonal measurements of the diameter are recorded, and the mean diameter is then used with the time it took for the spread to come to a stop, to calculate the yield stress value. The volume of the cone was calculated from the dimensions in Figure 2. The mean diameter of the spread and the final spread time including the volume of the cone was used to determine the yield stress by using Equation (2). This procedure was as described in the literature and conforms to the test procedure DIN 1164, and is in accordance with the Chinese standard GB/T 8077-2012 (2012) [3,20–31].

2.7.5. Total Organic Carbon Measurements

A Hach DR1900 spectrometer was used to determine the total organic carbon content (TOC) in order to determine the amount of polycarboxylate-based superplasticizer that adsorbed onto the cement particles. As the adsorption reaches saturation, un-adsorbed SP will remain in the medium and assist with fluidity. This was then used to determine the amount of SP before and after adsorption, using the depletion method [13,17,22,23,26,27,29,32–36].

2.7.6. Sample Preparations for the TOC Test

To prepare the sample for the TOC test, 0.25 g of SP was mixed with 44.75 g of water before adding the wet mixture to 100 g of dry cement. The fresh cement paste was mixed for 2 min to ensure full homogenization [37]. The fresh cement paste was immediately transferred to the centrifuge tube at a predetermined volume to ensure consistency. The cement paste was centrifuged at 3000–8000 r/min for 5 min to separate the solids from the liquids [17,29,33–35,37,38]. The supernatant was removed with a glass syringe and the sample was stored in a glass vial. The sample was then diluted 5-fold in order to reach the reading range of the TOC analyzer [12]. Two mL of the sample and 8 mL of deionized TOC-free water was added to a 100 mL volumetric flask (2 mL sample + 8 mL of deionized water) and homogenized with a stirrer bar for 5 min.

3. Results

The rheological behavior of cement pastes was assessed using different techniques, such as empirical and rheometric approaches, to respectively evaluate the loss in workability (yield stress evolution) and the fresh property of the cement paste. It was important to confirm these two approaches to establish confidence in the results. The yield stress values obtained from the rheometer and the mini-slump test correlated very well, as shown in Figure 3 ($R^2 = 0.98$).

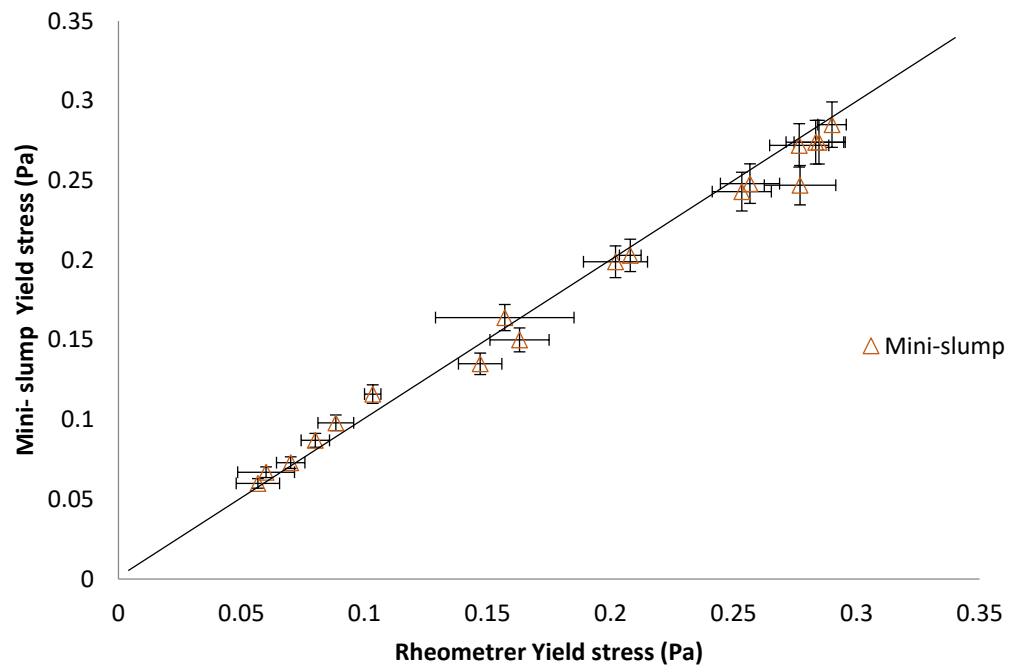


Figure 3. Correlation between the yield stresses determined using a mini-slump test and rheometer with the blended SP at optimum dosage with different proportions of SP-A and SP-B, for Cement 1, Cement 2 and Cement 3.

This strong correlation has been published in the literature showing that empirical tests, such as the mini-slump test, is adequate for determining the initial yield stress of low viscosity cement pastes [3,33]. This provides confidence for using the mini-slump flow test as rapid tests to assess rheological behavior of cementitious materials for fast adjustments on sites where more sophisticated instruments are not available.

3.1. Effect of SP-C Blend on the Yield Stress of Cement

The effectiveness of the blended SP, SP-C on the three cements' rheological behavior was assessed by evaluating the corresponding yield stress values with different proportions of SP-A and SP-B at the predetermined optimum dosage as shown in Figure 4.

It was assumed that the different responses in yield stress values as per Figure 4 for the three cements would result from the differences in their characteristics. It could be observed that SP-C does not have much effect on Cement 3 until the SP-A fraction is increased above 50% in the blend. For Cement 3, SP-C only starts to affect the yield stress of the corresponding cement paste at higher fractions of SP-A. However, for cement C1, SP-C can be seen to continuously decrease its yield stress at lower fractions of SP-A below 50% and remains unaffected when further increased. A slight decrease in the trend of the yield stress was observed for Cement 2 as the SP-A fraction within SP-C increases.

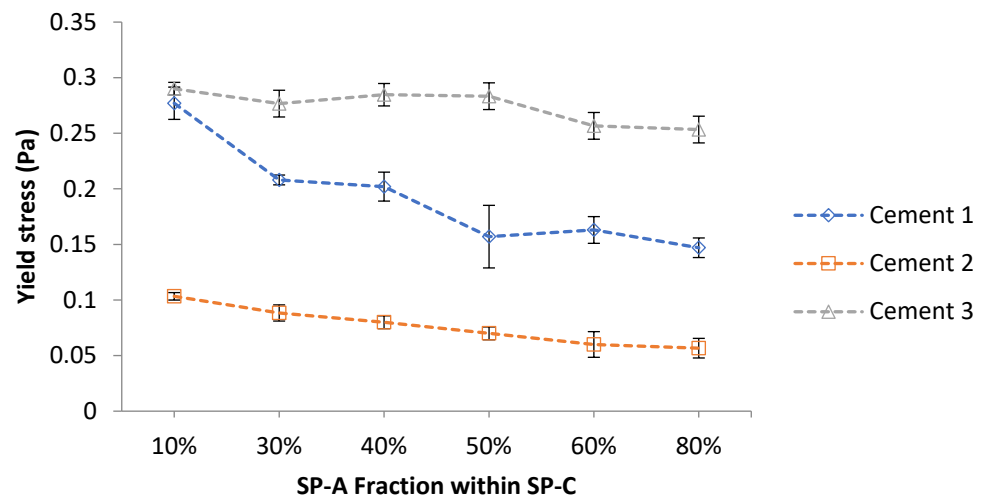


Figure 4. Summary of the yield stress (Pa) values of Cement 1, Cement 2 and Cement 3 with SP-C expressed as a fraction of SP-A at optimum dosage of 0.25%.

3.2. The Effect of the SP-C Blend on the Viscosity of the Cement

The viscosity of Cement 3 in Figure 5 is seen to increase, as the SP-A fraction within SP-B increases over the whole range by approximately 40%. This increase in viscosity can be linked to the entanglement of polymers. However, the viscosities of Cement 1 and Cement 2 remained fairly constant at increased dosages of SP-A. This shows that the optimum dosage was effective because the yield stress values of all three cements were affected differently at optimum dosage, where at the same dosage, the viscosity was only slightly affected and even increased as in the case of Cement 3.

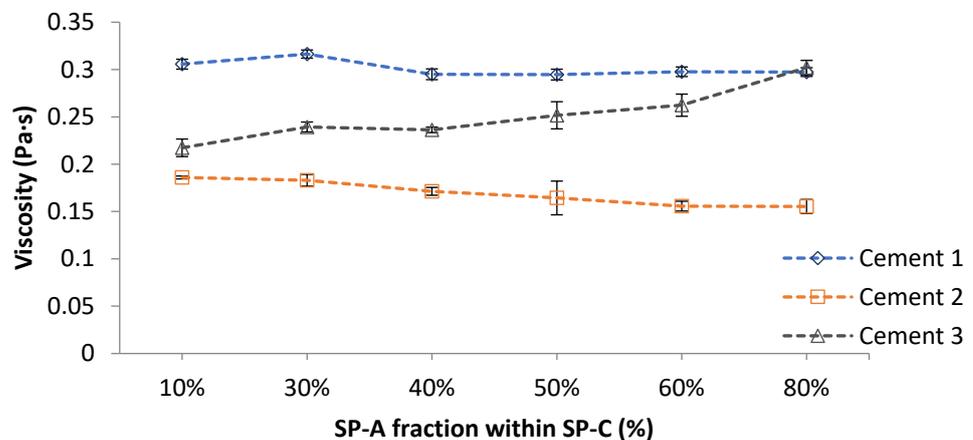


Figure 5. Summary of the plastic viscosity (Pa·s) of Cement 1, Cement 2 and Cement 3 with the addition of SP-C at 0.25%.

3.3. The Effect of SP-C Blend on the Adsorption

The adsorption ability of blended SP-C on cement particles within cement systems were assessed for the three different cements (Figure 6). It was observed that at any SP-A fraction content, SP-C exhibited a higher SP adsorption ability in Cement 3, followed by Cement 1. In comparison, Cement 2 demonstrated the lowest SP-C adsorption ability for all SP-A fractions.

Cement 1, which is coarser, theoretically should adsorb less SP, and with a low sulphate and alkali equivalent, favors the dissolution of Ca-ions. This allows for the adsorption of SP on the cement without the competitiveness of sulphate ions.

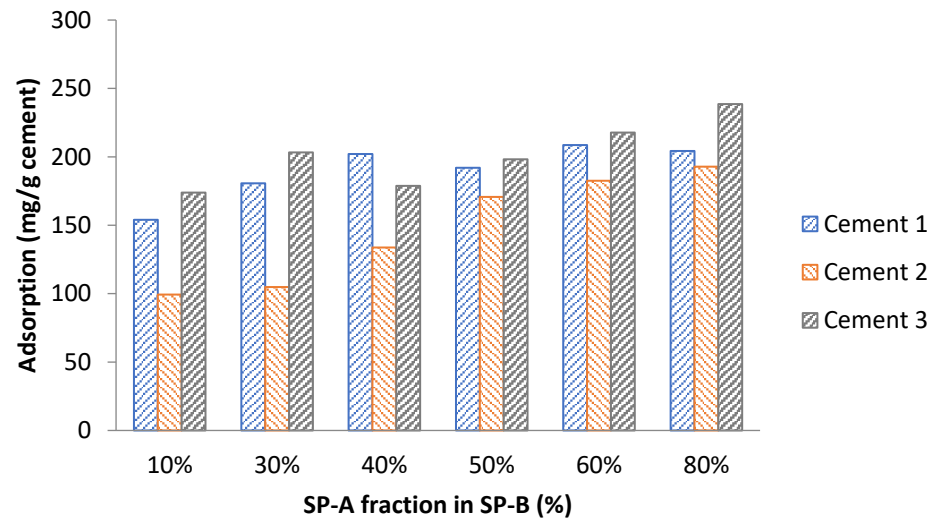


Figure 6. Summary of the adsorption (mg/g cement) of SP-C at 0.25% on Cement 1, Cement 2 and Cement 3.

Cement 2, which is finer (theoretically should adsorb more SP), released higher sulphate ions, which was favored by the higher alkali content. This resulted in less SP-A needed in the blend SP-C to reach its hydrophilicity.

Cement 3, which is finer and expected to adsorb more SP, was justified by the higher adsorption results. The lack of Ca-ions for sulphate ion reaction favors more SP adsorption to the cement. The slow release of Ca-ions is exacerbated by the low alkali content in the cement.

4. Discussion

The strong correlation observed between the empirical and rheometric measurements was more pronounced for cement systems with a low viscosity. This was in line with the finding reported in [3,21,33]. From the results presented in Section 3, the affinity of the blended SP-C was more supported by the amount of SP-A content within the blend. Since SP-A ionic charges were higher than that of SP-B, it could be assumed that when two admixtures are blended and added to a cement system, the admixture possessing the highest average anionic charge density will have the priority in adsorbing to the cement particles. The capacity of an SP in reducing the rheological parameter values could not only be attributed to its adsorption amount, but also to the length of the side chains. This is because the longer the side chains of the polymer, the greater the steric hindrance it can provide; therefore, increasing the fluidity of the cement paste [1,27]. Moreover, the competitive adsorption behavior of SPs within a cement system could also be affected by sulphate ions, thus altering the efficiency of the SP [32].

In fact, the ratio between the sulphate content and aluminate phase is one of the key parameters in regulating the SP effectiveness. It has been shown that a sulphate/C₃A ratio between 0.7 and 2.0 was sufficient for aluminate hydrate growth and could prevent the production of organo-mineral phases, which formation requires large amounts of SP consumption [18]. Cement 1 and Cement 3 demonstrated higher adsorption abilities than Cement 2 at all concentrations of SP-A fractions, probably due to their higher C₃A phases that reacted with the corresponding sulphate phases and led to higher ratio values that imply important SP consumption. In contrast, their yield stress values were higher, confirming that the consumed SP within these cements were used more to produce organo-mineral phases than for particle repulsion.

The chemical composition of the investigated cements played an important role in affecting their fresh property. Probably, the lower sulphate and alkali contents in Cement 1 favored the dissolution of Ca-ions resulting in greater SP adsorption onto the cement particles without the competitiveness of sulphate ions. For the higher concentration of

sulphate in Cement 2, whose adsorption was favored by a high alkali content, slowed down the adsorption of SP onto the reactive cement sites. The slow release of Ca-ions, due to the low alkali content and the low concentration of sulphate ions in Cement 3, favored the SP adsorption onto the cement.

The rheological performances of cement pastes were in line with the adsorption behavior of the blended SP-C. Cement 1 with lower adsorption ability, especially at low SP-A contents, resulted in lower yield stress values. This would assume that the excess SP within the system repulsed cement particles through the hindrance effect phenomenon and, therefore, increased the fluidity of the mix demonstrated by low viscosity values.

It is quite clear that the effectiveness of the SP, as shown in Figures 4 and 5, could be achieved by blending the PCE-based SP with short side chains and different molecular masses for rheological improvements of the mix. This is instrumental to ensure that un-adsorbed polymer remaining in the medium has an opportunity to assist in increasing the fluidity within the medium, as the polymer with a higher molecular weight gets preference in adsorbing first, saturating the adsorption sites before getting consumed by the hydration products. It is after this consumption of the initially adsorbed polymer that the un-adsorbed polymer is given an opportunity to adsorb on the cement particle, which improves the fresh properties of the paste.

5. Conclusions

It has been shown that it is possible to blend a PCE SP to produce an SCC with the intention to achieve a desired rheological behavior. In this work, the effect of a blended PCE SP on the rheology of SCCP using three cements with different chemical compositions was investigated. Considering that aggregates are inert materials within the cement system, the observed trends could be expected to be the same at the concrete scale.

It was observed that having two PCE SPs with same molecular structures, but with different weight and side chain length, could be blended for tailoring the rheological behavior of self-compacting concretes. This can be achieved because SPs with higher molecular weights absorb first to the cement particles giving those with lower molecular weights an opportunity to adsorb later thus increasing the fluidity of the system. It is, therefore, possible to obtain a new SP with improved properties, blending different agents by varying fractions to control the flow properties of a cement system.

Although it is common practice for SP suppliers to blend PCE SPs to achieve certain rheological properties of cement systems, this study helps to better understand the effect and behavior of blended PCE SP cement systems to help improve the design of SCC mixes within concrete technology.

Author Contributions: Methodology, W.M.; Formal analysis, M.S.; Investigation, M.S.; Writing—original draft, M.S.; Writing—review & editing, M.S., W.M. and R.H.; Visualization, M.S. and W.M.; Supervision, W.M. and R.H.; Project administration, R.H. All authors have read and agreed to the published version of the manuscript.

Funding: This research received no external funding.

Institutional Review Board Statement: Not applicable.

Informed Consent Statement: Not applicable.

Data Availability Statement: The data used in this article is available in the CPUT library repository which forms part of the masters project of M.S.

Acknowledgments: This work was supported by the Flow Process and Rheology Centre, Cape Peninsula University of Technology.

Conflicts of Interest: The authors declare no conflict of interest.

References

1. Banfill, P.F.G. Additivity effects in the rheology of fresh concrete containing water-reducing admixtures. *Constr. Build. Mater.* **2011**, *25*, 2955–2960. [[CrossRef](#)]
2. González-Taboada, I.; González-Fontebo, B.; Eiras-López, J.; Rojo-López, G. Tools for the study of self-compacting recycled concrete fresh behaviour: Workability and rheology. *J. Clean. Prod.* **2017**, *156*, 1–18. [[CrossRef](#)]
3. Dalas, F.; Pourchet, S.; Nonat, A.; Rinaldi, D.; Sabio, S.; Mosquet, M. Fluidizing efficiency of comb-like superplasticizers: The effect of the anionic function, the side chain length and the grafting degree. *Cem. Concr. Res.* **2015**, *71*, 115–123. [[CrossRef](#)]
4. Xie, J.; Kayali, O. Effect of superplasticiser on workability enhancement of Class F and Class C fly ash-based geopolymers. *Constr. Build. Mater.* **2016**, *122*, 36–42. [[CrossRef](#)]
5. Zhang, Y.; Kong, X. Correlations of the dispersing capability of NSF and PCE types of superplasticizer and their impacts on cement hydration with the adsorption in fresh cement pastes. *Cem. Concr. Res.* **2015**, *69*, 1–9. [[CrossRef](#)]
6. Ramalingam, M.; Narayanan, K.; Sivamani, J.; Kathirvel, P.; Murali, G.; Vatin, N.I. Experimental Investigation on the Potential Use of Magnetic Water as a Water Reducing Agent in High Strength Concrete. *Materials* **2022**, *15*, 5219. [[CrossRef](#)] [[PubMed](#)]
7. Plank, J.; Pöllmann, K.; Zouaoui, N.; Andres, P.; Schaefer, C. Synthesis and performance of methacrylic ester based polycarboxylate superplasticizers possessing hydroxy terminated poly(ethylene glycol) side chains. *Cem. Concr. Res.* **2008**, *38*, 1210–1216. [[CrossRef](#)]
8. Lange, A.; Hirata, T.; Plank, J. Influence of the HLB value of polycarboxylate superplasticizers on the flow behavior of mortar and concrete. *Cem. Concr. Res.* **2014**, *60*, 45–50. [[CrossRef](#)]
9. Plank, J.; Sachsenhauser, B. Experimental determination of the effective anionic charge density of polycarboxylate superplasticizers in cement pore solution. *Cem. Concr. Res.* **2009**, *39*, 1–5. [[CrossRef](#)]
10. Tan, H.; Zou, F.; Ma, B.; Liu, M.; Li, X.; Jian, S. Effect of sodium tripolyphosphate on adsorbing behavior of polycarboxylate superplasticizer. *Constr. Build. Mater.* **2016**, *126*, 617–623. [[CrossRef](#)]
11. Alonso, M.; Puertas, F. Adsorption of PCE and PNS superplasticisers on cubic and orthorhombic C3A. Effect of sulfate. *Constr. Build. Mater.* **2015**, *78*, 324–332. [[CrossRef](#)]
12. Li, G.; He, T.; Hu, D.; Shi, C. Effects of two retarders on the fluidity of pastes plasticized with aminosulfonic acid-based superplasticizers. *Constr. Build. Mater.* **2011**, *26*, 72–78. [[CrossRef](#)]
13. Plank, J.; Winter, C. Competitive adsorption between superplasticizer and retarder molecules on mineral binder surface. *Cem. Concr. Res.* **2008**, *38*, 599–605. [[CrossRef](#)]
14. Yoon, J.Y.; Kim, J.H. Evaluation on the consumption and performance of polycarboxylates in cement-based materials. *Constr. Build. Mater.* **2018**, *158*, 423–431. [[CrossRef](#)]
15. Bey, H.B.; Hot, J.; Baumann, R.; Roussel, N. Consequences of competitive adsorption between polymers on the rheological behaviour of cement pastes. *Cem. Concr. Compos.* **2014**, *54*, 17–20. [[CrossRef](#)]
16. Matsuzawa, K.; Shimazaki, D.; Kawakami, H.; Sakai, E. Effect of non-adsorbed superplasticizer molecules on fluidity of cement paste at low water-powder ratio. *Cem. Concr. Compos.* **2019**, *97*, 218–225. [[CrossRef](#)]
17. Janowska-Renkas, E. The effect of superplasticizers' chemical structure on their efficiency in cement pastes. *Constr. Build. Mater.* **2013**, *38*, 1204–1210. [[CrossRef](#)]
18. Erzençin, S.G.; Kaya, K.; Özkorucuklu, S.P.; Özdemir, V.; Yıldırım, G. The properties of cement systems superplasticized with methacrylic ester-based polycarboxylates. *Constr. Build. Mater.* **2018**, *166*, 96–109. [[CrossRef](#)]
19. He, Y.; Zhang, X.; Shui, L.; Wang, Y.; Gu, M.; Wang, X.; Wang, H.; Peng, L. Effects of PCEs with various carboxylic densities and functional groups on the fluidity and hydration performances of cement paste. *Constr. Build. Mater.* **2019**, *202*, 656–668. [[CrossRef](#)]
20. Zhang, K.; Pan, L.; Li, J.; Lin, C.; Cao, Y.; Xu, N.; Pang, S. How does adsorption behavior of polycarboxylate superplasticizer effect rheology and flowability of cement paste with polypropylene fiber? *Cem. Concr. Compos.* **2019**, *95*, 228–236. [[CrossRef](#)]
21. Chomyn, C.; Plank, J. Impact of different synthesis methods on the dispersing effectiveness of isoprenol ether-based zwitterionic and anionic polycarboxylate (PCE) superplasticizers. *Cem. Concr. Res.* **2019**, *119*, 113–125. [[CrossRef](#)]
22. Dalas, F.; Nonat, A.; Pourchet, S.; Mosquet, M.; Rinaldi, D.; Sabio, S. Tailoring the anionic function and the side chains of comb-like superplasticizers to improve their adsorption. *Cem. Concr. Res.* **2015**, *67*, 21–30. [[CrossRef](#)]
23. Lange, A.; Plank, J. Contribution of non-adsorbing polymers to cement dispersion. *Cem. Concr. Res.* **2016**, *79*, 131–136. [[CrossRef](#)]
24. Lin, X.; Liao, B.; Zhang, J.; Li, S.; Huang, J.; Pang, H. Synthesis and characterization of high-performance cross-linked polycarboxylate superplasticizers. *Constr. Build. Mater.* **2019**, *210*, 162–171. [[CrossRef](#)]
25. Liu, X.; Guan, J.; Lai, G.; Zheng, Y.; Wang, Z.; Cui, S.; Lan, M.; Li, H. Novel designs of polycarboxylate superplasticizers for improving resistance in clay-contaminated concrete. *J. Ind. Eng. Chem.* **2017**, *55*, 80–90. [[CrossRef](#)]
26. Liu, X.; Guan, J.; Lai, G.; Wang, Z.; Zhu, J.; Cui, S.; Lan, M.; Li, H. Performances and working mechanism of a novel polycarboxylate superplasticizer synthesized through changing molecular topological structure. *J. Colloid Interface Sci.* **2017**, *504*, 12–24. [[CrossRef](#)] [[PubMed](#)]
27. Marchon, D.; Boscaro, F.; Flatt, R.J. First steps to the molecular structure optimization of polycarboxylate ether superplasticizers: Mastering fluidity and retardation. *Cem. Concr. Res.* **2019**, *115*, 116–123. [[CrossRef](#)]
28. Qian, S.; Yao, Y.; Wang, Z.; Cui, S.; Liu, X.; Jiang, H.; Guo, Z.; Lai, G.; Xu, Q.; Guan, J. Synthesis, characterization and working mechanism of a novel polycarboxylate superplasticizer for concrete possessing reduced viscosity. *Constr. Build. Mater.* **2018**, *169*, 452–461. [[CrossRef](#)]

29. Tian, H.; Kong, X.; Su, T.; Wang, D. Comparative study of two PCE superplasticizers with varied charge density in Portland cement and sulfoaluminate cement systems. *Cem. Concr. Res.* **2019**, *115*, 43–58. [[CrossRef](#)]
30. Yang, Z.; Yu, M.; Liu, Y.; Chen, X.; Zhao, Y. Synthesis and performance of an environmentally friendly polycarboxylate superplasticizer based on modified poly(aspartic acid). *Constr. Build. Mater.* **2019**, *202*, 154–161. [[CrossRef](#)]
31. Zhang, Y.; Kong, X.; Gao, L.; Bai, Y. Characterization of the mesostructural organization of cement particles in fresh cement paste. *Constr. Build. Mater.* **2016**, *124*, 1038–1050. [[CrossRef](#)]
32. Zhu, Q.-H.; Zhang, L.-Z.; Min, X.-M.; Yu, Y.-X.; Zhao, X.-F.; Li, J.-H. Comb-typed polycarboxylate superplasticizer equipped with hyperbranched polyamide teeth. *Colloids Surf. A Physicochem. Eng. Asp.* **2018**, *553*, 272–277. [[CrossRef](#)]
33. Bessaies-Bey, H.; Baumann, R.; Schmitz, M.; Radler, M.; Roussel, N. Organic admixtures and cement particles: Competitive adsorption and its macroscopic rheological consequences. *Cem. Concr. Res.* **2016**, *80*, 1–9. [[CrossRef](#)]
34. Hot, J.; Bessaies-Bey, H.; Brumaud, C.; Duc, M.; Castella, C.; Roussel, N. Adsorbing polymers and viscosity of cement pastes. *Cem. Concr. Res.* **2014**, *63*, 12–19. [[CrossRef](#)]
35. Liu, X.; Wang, Z.; Zhu, J.; Zheng, Y.; Cui, S.; Lan, M.; Li, H. Synthesis, characterization and performance of a polycarboxylate superplasticizer with amide structure. *Colloids Surf. A Physicochem. Eng. Asp.* **2014**, *448*, 119–129. [[CrossRef](#)]
36. Zhang, Y.-R.; Cai, X.-P.; Kong, X.-M.; Gao, L. Effects of comb-shaped superplasticizers with different charge characteristics on the microstructure and properties of fresh cement pastes. *Constr. Build. Mater.* **2017**, *155*, 441–450. [[CrossRef](#)]
37. Zingg, A.; Winnefeld, F.; Holzer, L.; Pakusch, J.; Becker, S.; Figi, R.; Gauckler, L. Interaction of polycarboxylate-based superplasticizers with cements containing different C3A amounts. *Cem. Concr. Compos.* **2009**, *31*, 153–162. [[CrossRef](#)]
38. Lu, Z.; Kong, X.; Zhang, C.; Xing, F.; Cai, Y.; Jiang, L.; Zhang, Y.; Dong, B. Effect of surface modification of colloidal particles in polymer latexes on cement hydration. *Constr. Build. Mater.* **2017**, *155*, 1147–1157. [[CrossRef](#)]

Disclaimer/Publisher’s Note: The statements, opinions and data contained in all publications are solely those of the individual author(s) and contributor(s) and not of MDPI and/or the editor(s). MDPI and/or the editor(s) disclaim responsibility for any injury to people or property resulting from any ideas, methods, instructions or products referred to in the content.